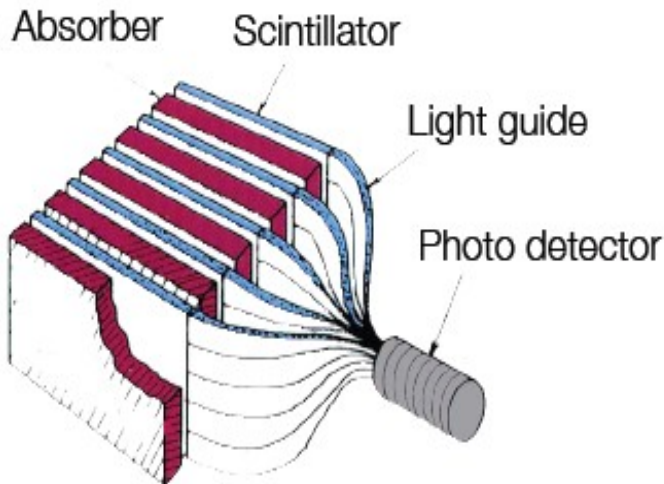
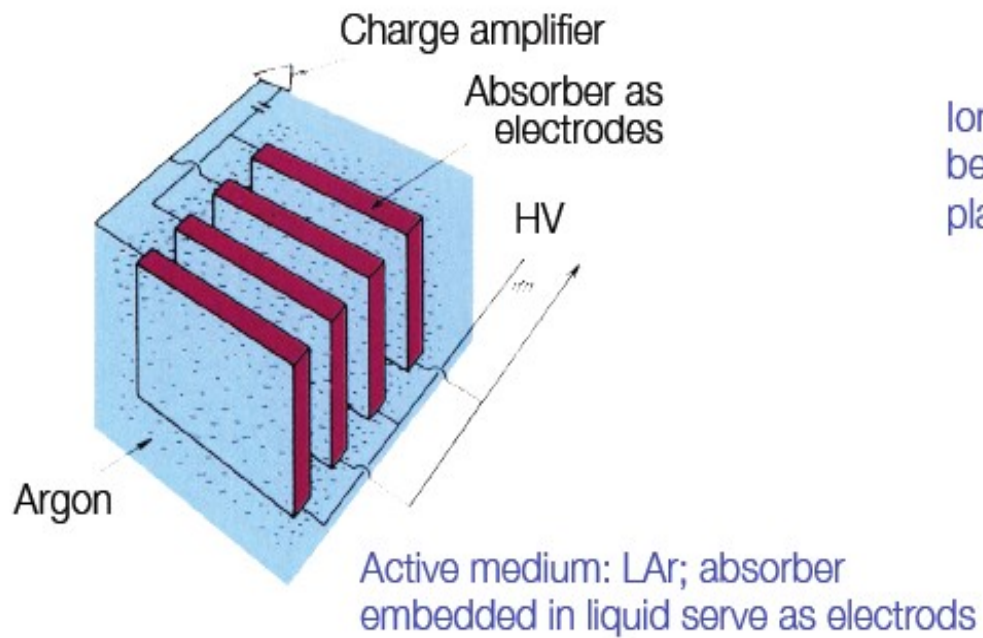
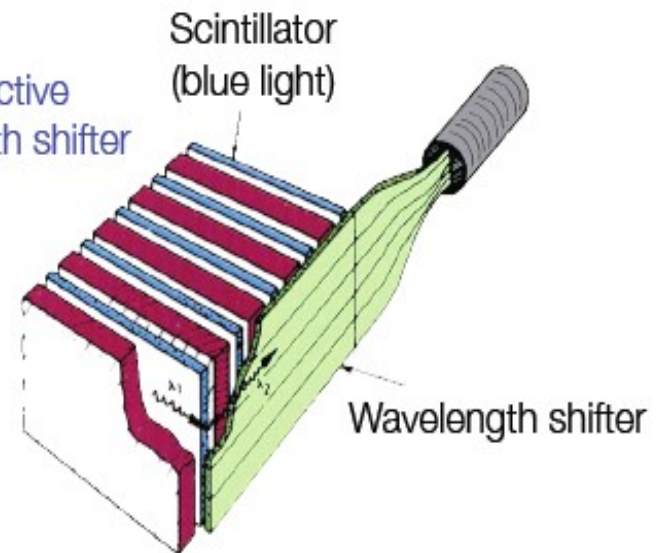


Possible setups

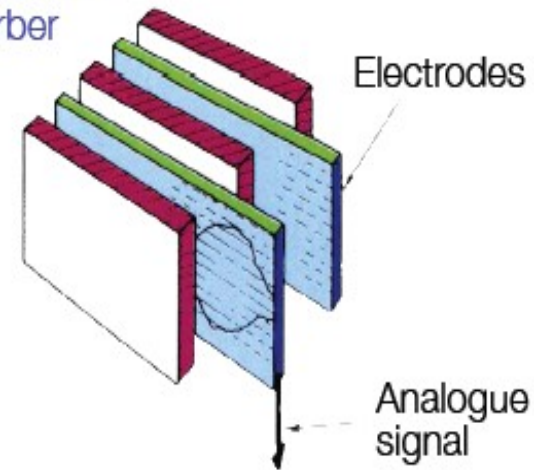
Scintillators as active layer;
signal readout via photo multipliers



Scintillators as active
layer; wave length shifter
to convert light



Ionization chambers
between absorber
plates



Reminder - Energy resolution of EM calorimeter

Intrinsic limit

Total number of track segments

$$N^{total} \propto \frac{E_0}{E_c}$$

Resolution

$$\frac{\sigma(E)}{E} \propto \frac{\sigma(N)}{N} \propto \frac{1}{\sqrt{N}} \propto \frac{1}{\sqrt{E_0}}$$

N – number of charged tracks

Spatial and angular resolution scale like $1/\sqrt{E}$

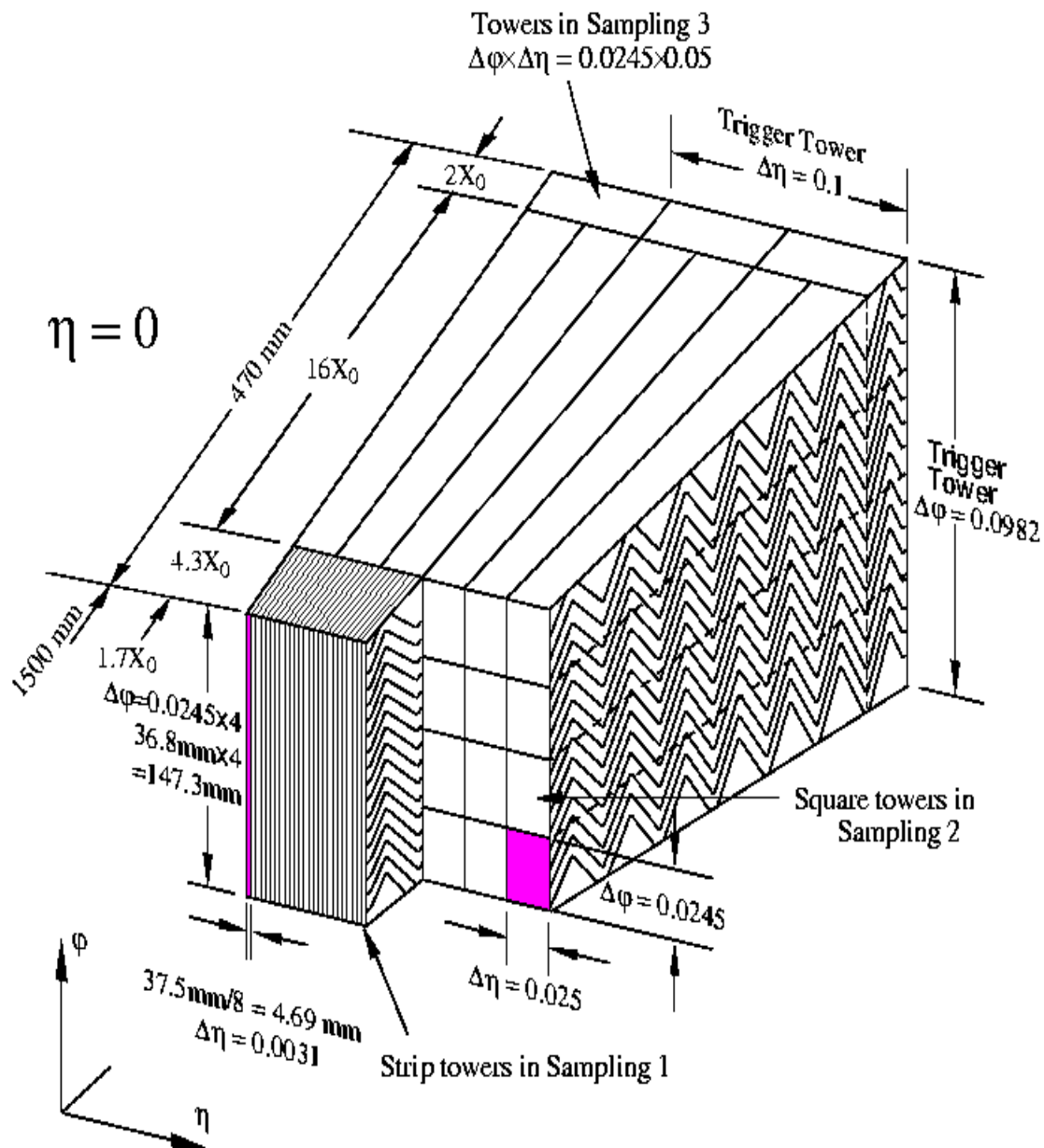
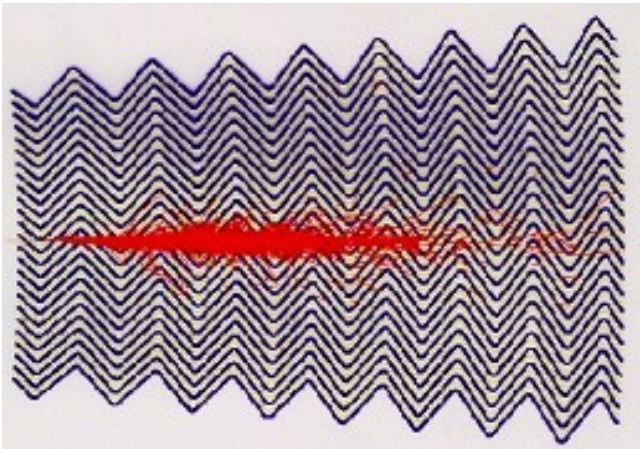
Relative energy resolution of a calorimeter improves with E_0

$$\frac{\sigma(E)}{E} = \frac{a}{\sqrt{E}} \oplus b \oplus \frac{c}{E}$$

stochastic term constant term noise term

inhomogeneities
bad cell inter-calibration
non-linearities

electronic noise
radioactivity
pile up



Hadron Showers

- Hadron calorimeter measurement
 - Charged hadrons: complementary to track measurement in magnetic field
 - Neutral hadrons: the only way to measure their energy.
- In nuclear collisions many secondary particles are produced
 - Secondary, tertiary nuclear reactions generate hadronic cascades
 - Electromagnetically decaying particles initiate EM showers

Both hadronic and electromagnetic showers are present

 - Energy can be absorbed as nuclear binding energy or target recoil (invisible energy)

Similar to EM showers, but more complex → need simulation tools (MC)

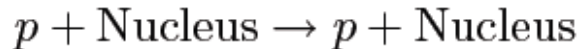
-→ GEANT

Characterized by the hadronic interaction length

Hadronic shower

Hadronic interaction:

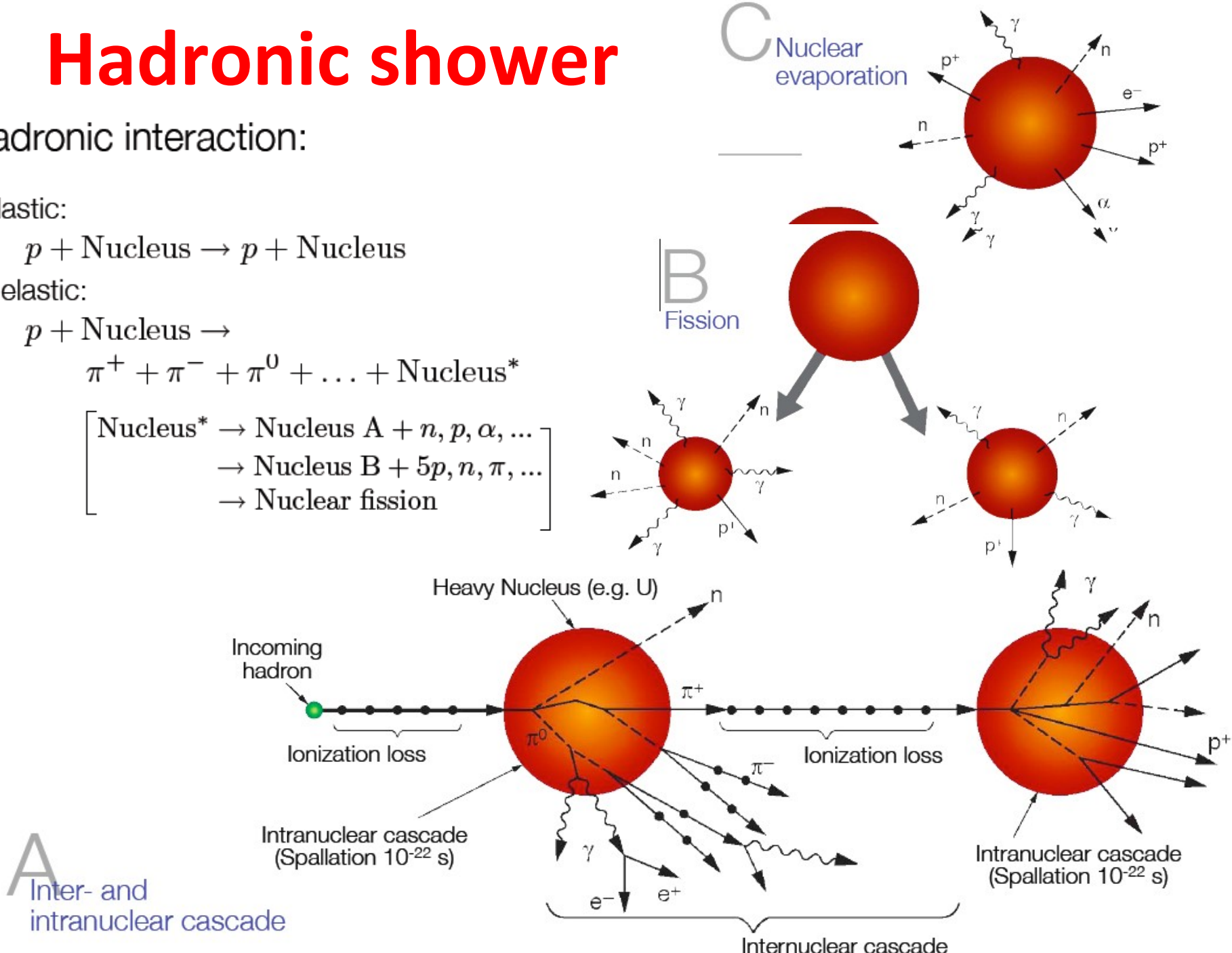
Elastic:

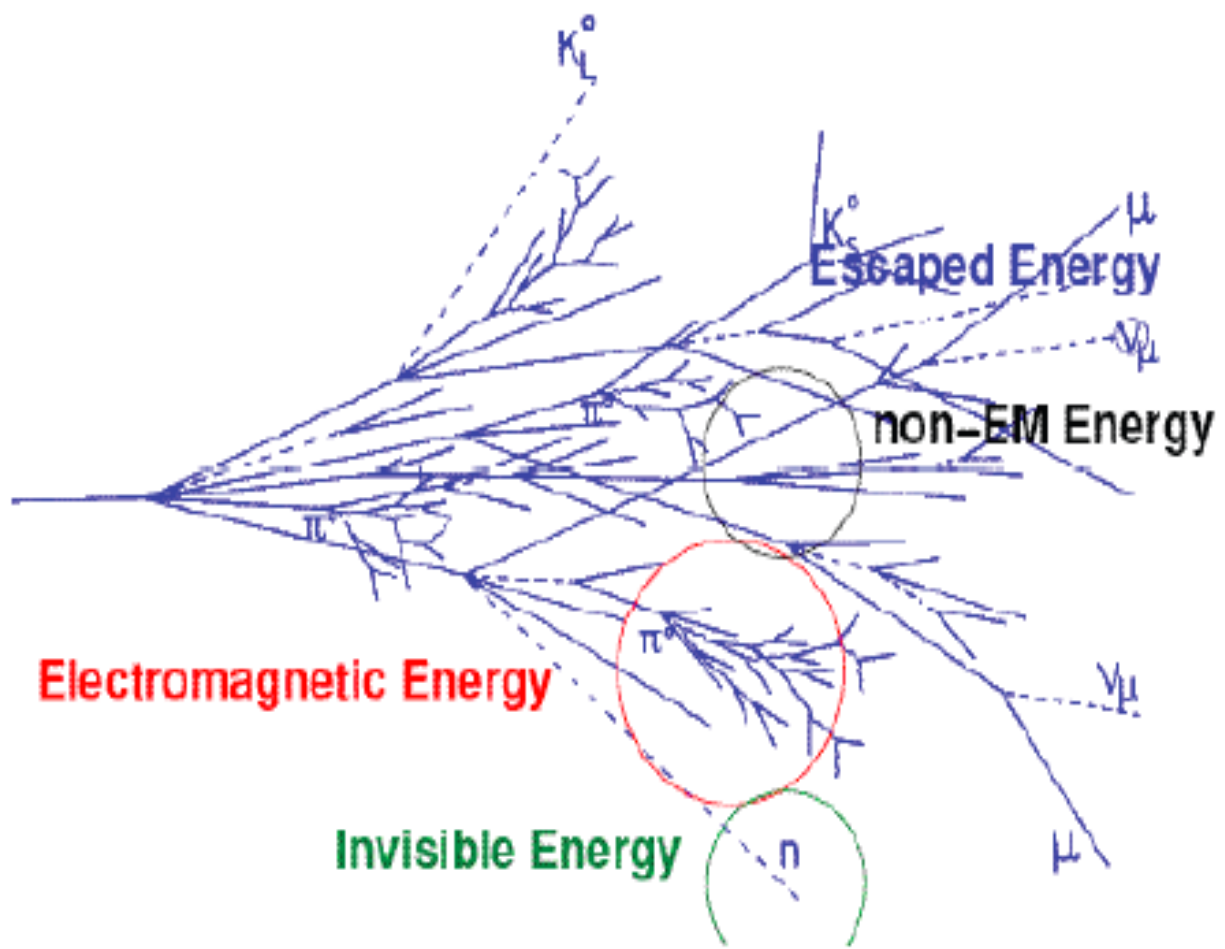


Inelastic:



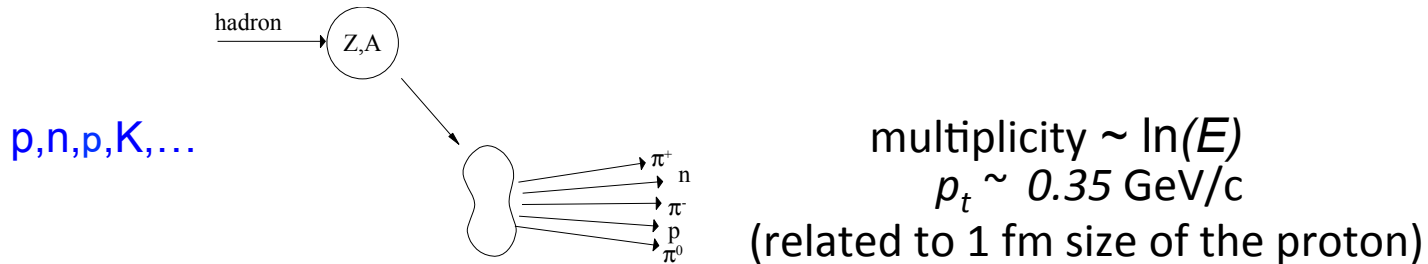
$\left[\begin{array}{l} \text{Nucleus}^* \rightarrow \text{Nucleus A} + n, p, \alpha, \dots \\ \rightarrow \text{Nucleus B} + 5p, n, \pi, \dots \\ \rightarrow \text{Nuclear fission} \end{array} \right]$





Nuclear interaction of hadrons

The interaction of energetic hadrons (charged or neutral) is determined by **inelastic nuclear processes**.



Excitation and breakup of nucleus \rightarrow nucleus fragments + secondary particles

At high energies ($>1 \text{ GeV}$) the cross-sections depend only weakly on the energy and on the type of the incident particle (p, p, K...)

$$\sigma_{inel} \approx \sigma_0 A^{0.7} \quad \sigma_{inel} (\text{pp at } 13 \text{ TeV}) \approx 73.1 \text{ mb}$$

In analogy to X_0 we define a **hadronic absorption length**

$$\lambda_a = \frac{A}{N_A \sigma_{inel}}$$

$$\lambda_{int} = \frac{1}{\sigma_{tot} \cdot n} = \frac{A \rho}{\sigma_{pp} A^{2/3} N_A} \approx \left(35 \text{ g/cm}^2 \right) A^{1/3}$$

$$N(x) = N(0) e^{-x/\lambda_{int}}$$

Hadronic shower

■ Hadronic

$$\sigma_{tot} = \sigma_{el} + \sigma_{inel}$$

$$\sigma_{el} \approx 10\text{mb} \quad \sigma_{inel} \approx A^{2/3}$$

$$\sigma_{tot} = \sigma_{tot}(pp)A^{2/3}$$

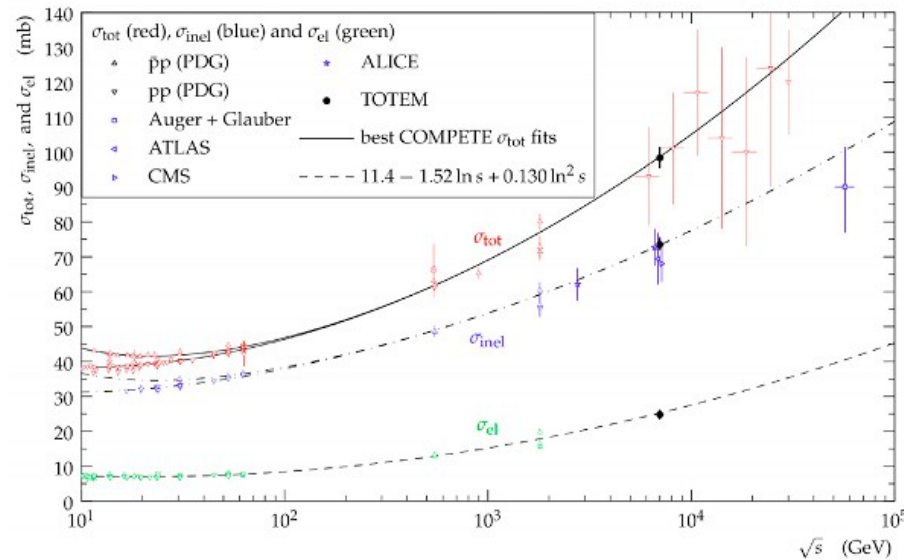
where: $\sigma_{tot}(pp)$ increases with \sqrt{s}

■ Hadronic

$$\lambda_{int} = \frac{1}{\sigma_{tot} \cdot n} = \frac{A\rho}{\sigma_{pp} A^{2/3} N_A} \approx (35\text{g/cm}^2)^{1/3}$$

$$N(x) = N(0)e^{-x/\lambda_{int}}$$

The geometric cross section is proportional to the square of the size of the nucleus A
 Nuclear radius scales as $A \sim A^{1/3} \rightarrow$ the nuclear mean free path in $\text{g/cm}^2 \sim A^{1/3}$.



■ λ_{int} characterizes both longitudinal and transverse shower profile

Hadronic interactions cross sections

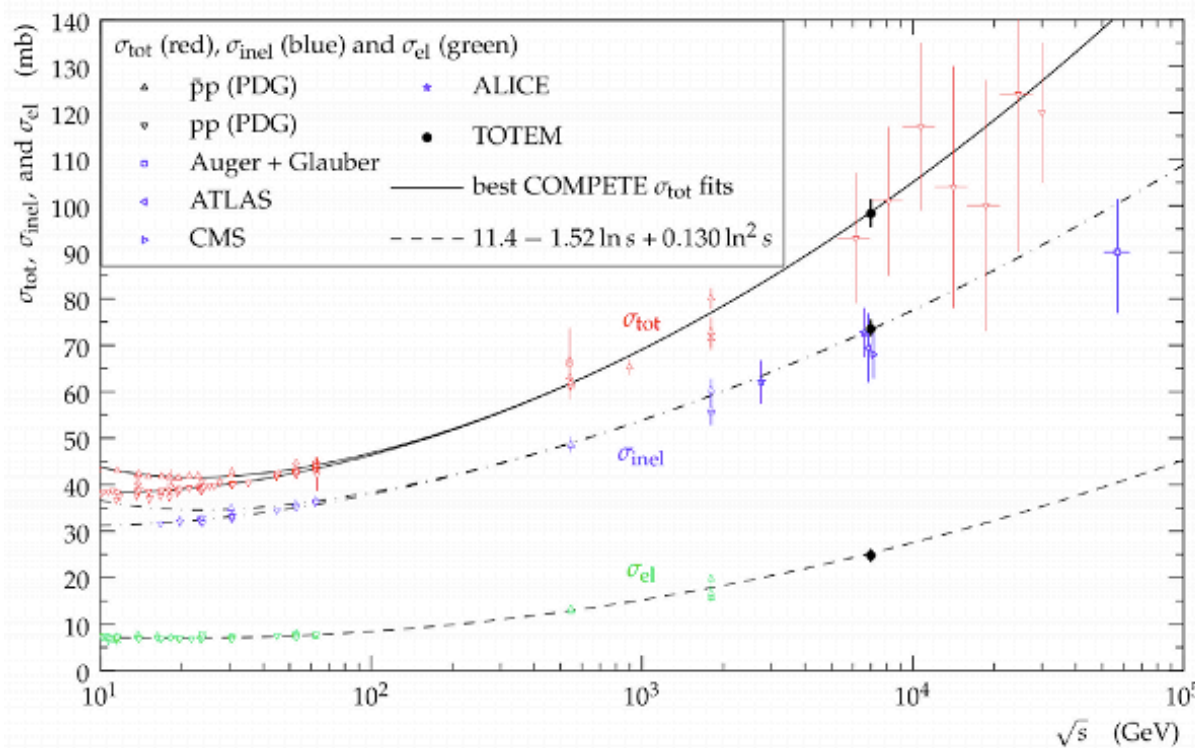
$$\sigma_{tot} = \sigma_{el} + \sigma_{inel}$$

$$\sigma_{el} \approx 10\text{mb}$$

$$\sigma_{inel} \approx A^{2/3}$$

$$\sigma_{tot}(nucl) = \sigma_{tot}(pp)A^{2/3}$$

$\sigma_{tot}(pp)$ increases with s

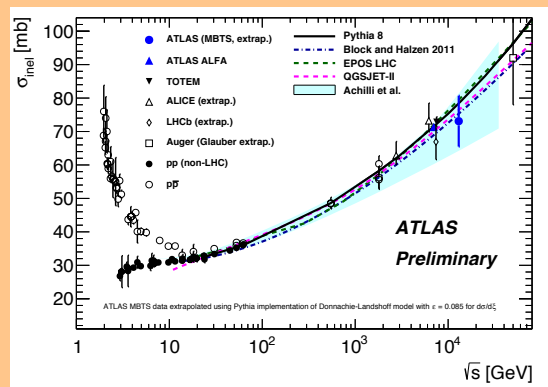
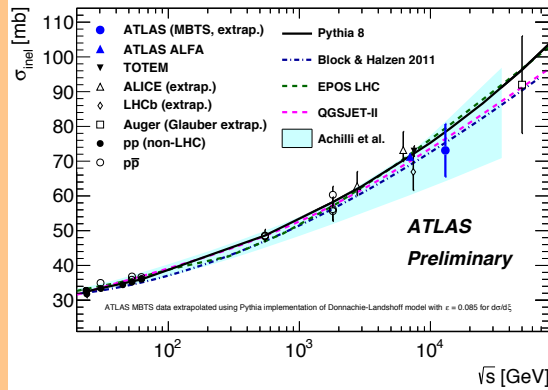


Note: Interactions include elastic scattering, where original hadron is free to interact again

QCD – basic properties of pp collisions

Early studies address global characteristics of events at 13 TeV

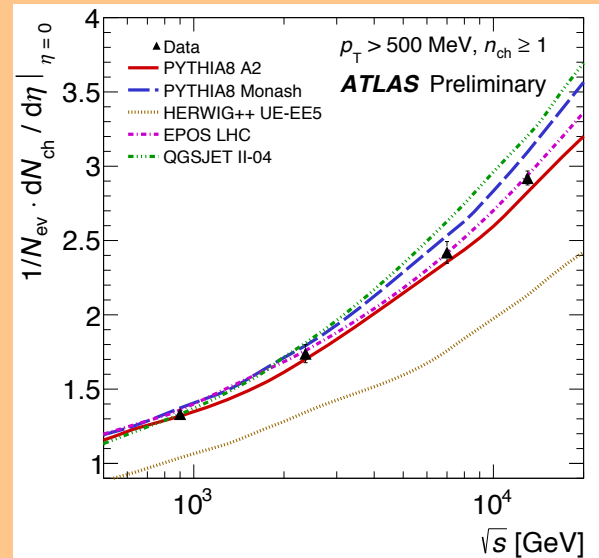
Inelastic cross section



ATLAS-CONF-2015-038

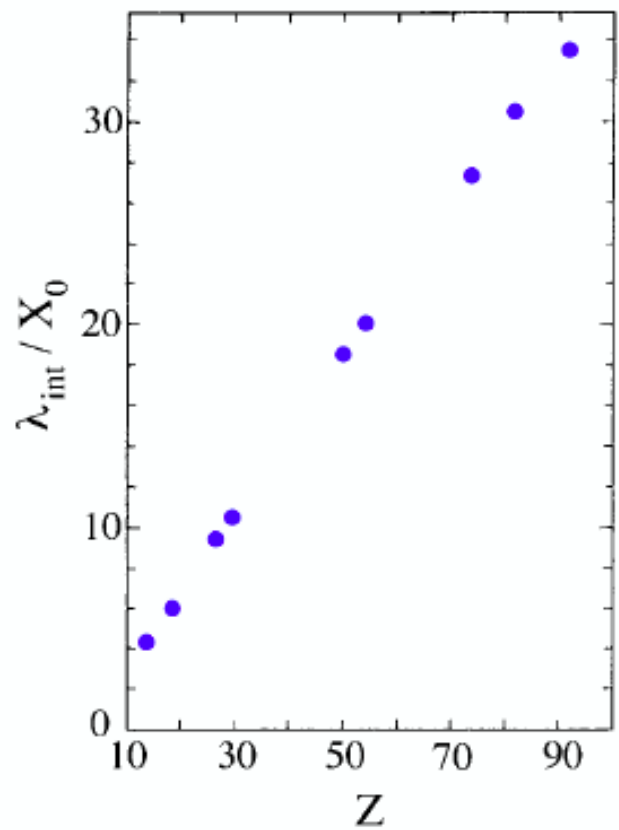
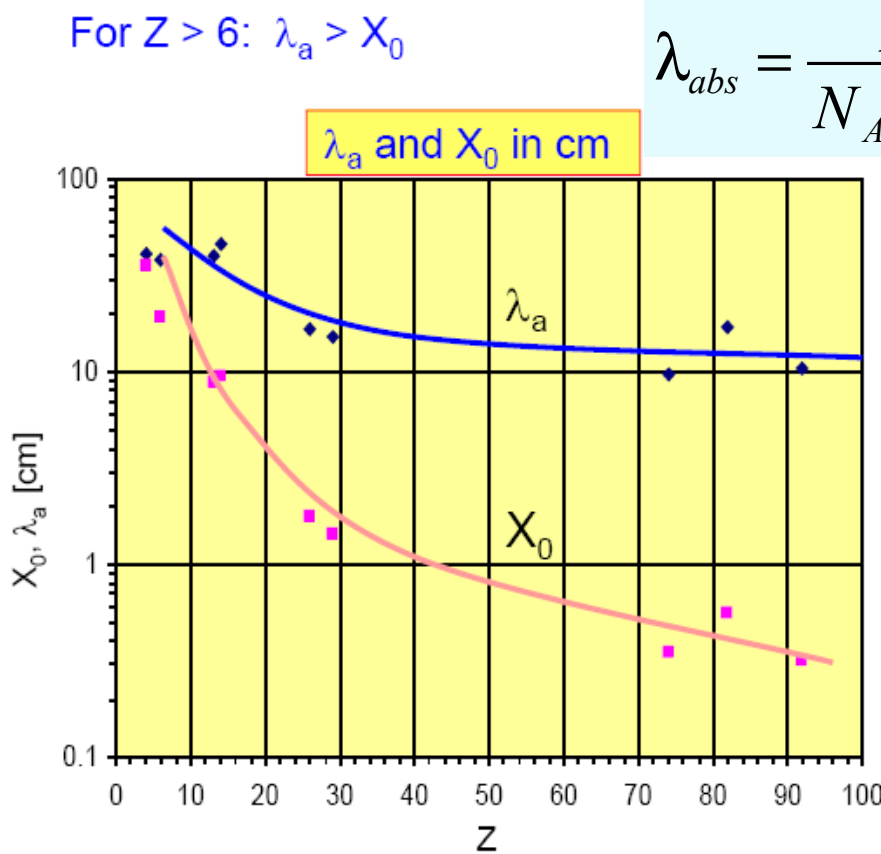
$$\sigma_{\text{TOT}}(13 \text{ TeV}) = 73.1 \pm 0.9 \text{ (exp)} \pm 0.9 \text{ (lum)} \pm 3.8 \text{ (extr)} \text{ mb}$$

Charged particle multiplicity



EPOS provides best description

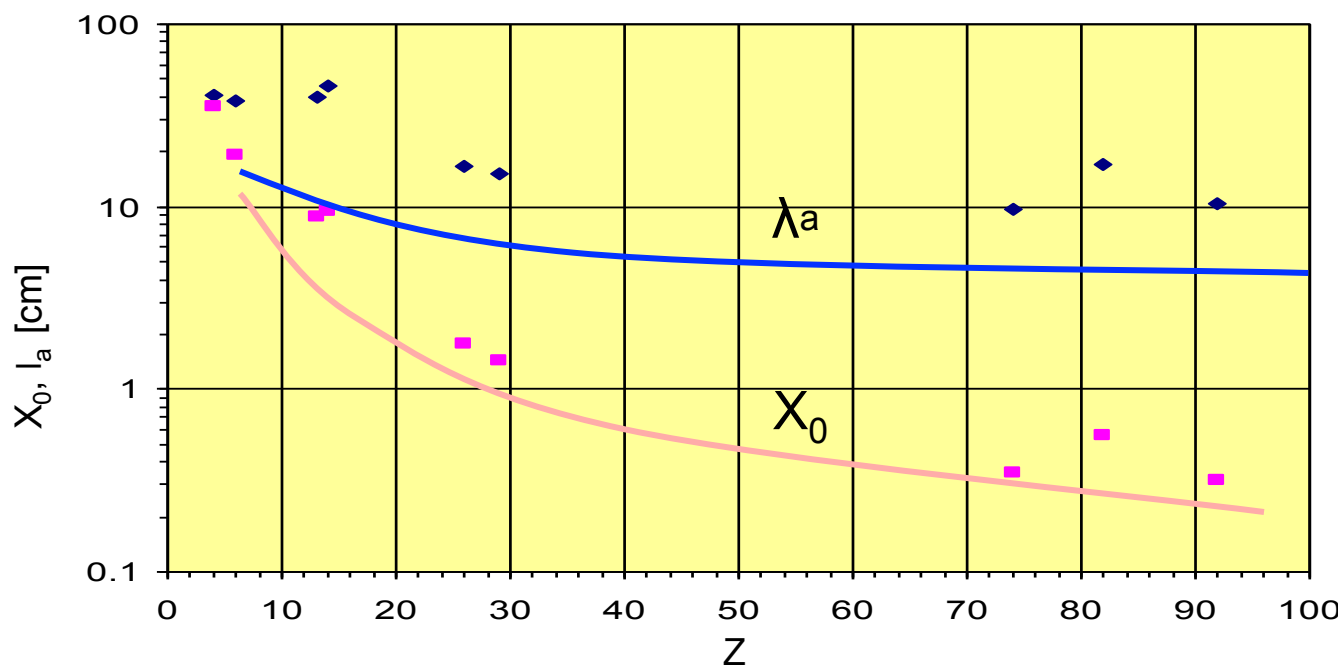
Material dependence



Radiation and absorption length

Material	Z	A	ρ [g/cm ³]	X_0 [g/cm ²]	λ_a [g/cm ²]
Hydrogen (gas)	1	1.01	0.0899 (g/l)	63	50.8
Helium (gas)	2	4.00	0.1786 (g/l)	94	65.1
Beryllium	4	9.01	1.848	65.19	75.2
Carbon	6	12.01	2.265	43	86.3
Nitrogen (gas)	7	14.01	1.25 (g/l)	38	87.8
Oxygen (gas)	8	16.00	1.428 (g/l)	34	91.0
Aluminium	13	26.98		2.7	106.4
Silicon	14	28.09		2.33	106.0
Iron	26	55.85		7.87	131.9
Copper	29	63.55		8.96	134.9
Tungsten	74	183.85		19.3	185.0
Lead	82	207.19		11.35	194.0
Uranium	92	238.03		18.95	199.0

For $Z > 6$: $\lambda_a > X_0$



Hadronic vs EM showers

Hadronic vs. electromagnetic interaction length:

$$\left. \begin{aligned} X_0 &\sim \frac{A}{Z^2} \\ \lambda_{\text{int}} &\sim A^{1/3} \end{aligned} \right] \rightarrow \frac{\lambda_{\text{int}}}{X_0} \sim A^{4/3}$$

$$\lambda_{\text{int}} \gg X_0$$

[$\lambda_{\text{int}}/X_0 > 30$ possible; see below]

Typical
Longitudinal size: 6 ... 9 λ_{int}
[95% containment]

[EM: 15-20 X_0]

Typical
Transverse size: one λ_{int}
[95% containment]

[EM: 2 R_M ; compact]

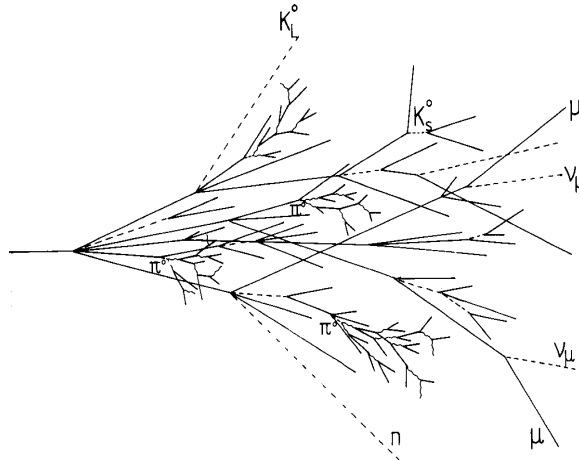
Some numerical values for materials typical used in hadron calorimeters

	λ_{int} [cm]	X_0 [cm]
Szint.	79.4	42.2
LAr	83.7	14.0
Fe	16.8	1.76
Pb	17.1	0.56
U	10.5	0.32
C	38.1	18.8

Hadronic calorimeter need more depth than electromagnetic calorimeter ...

Hadronic cascades

Various processes involved. Much more complex than electromagnetic cascades.



hadronic



charged pions, protons, kaons

breaking up of nuclei (binding energy),

neutrons, neutrinos, soft g' s

muons -> invisible energy

$$n(\pi^0) \approx \ln E(\text{GeV}) - 4.6$$

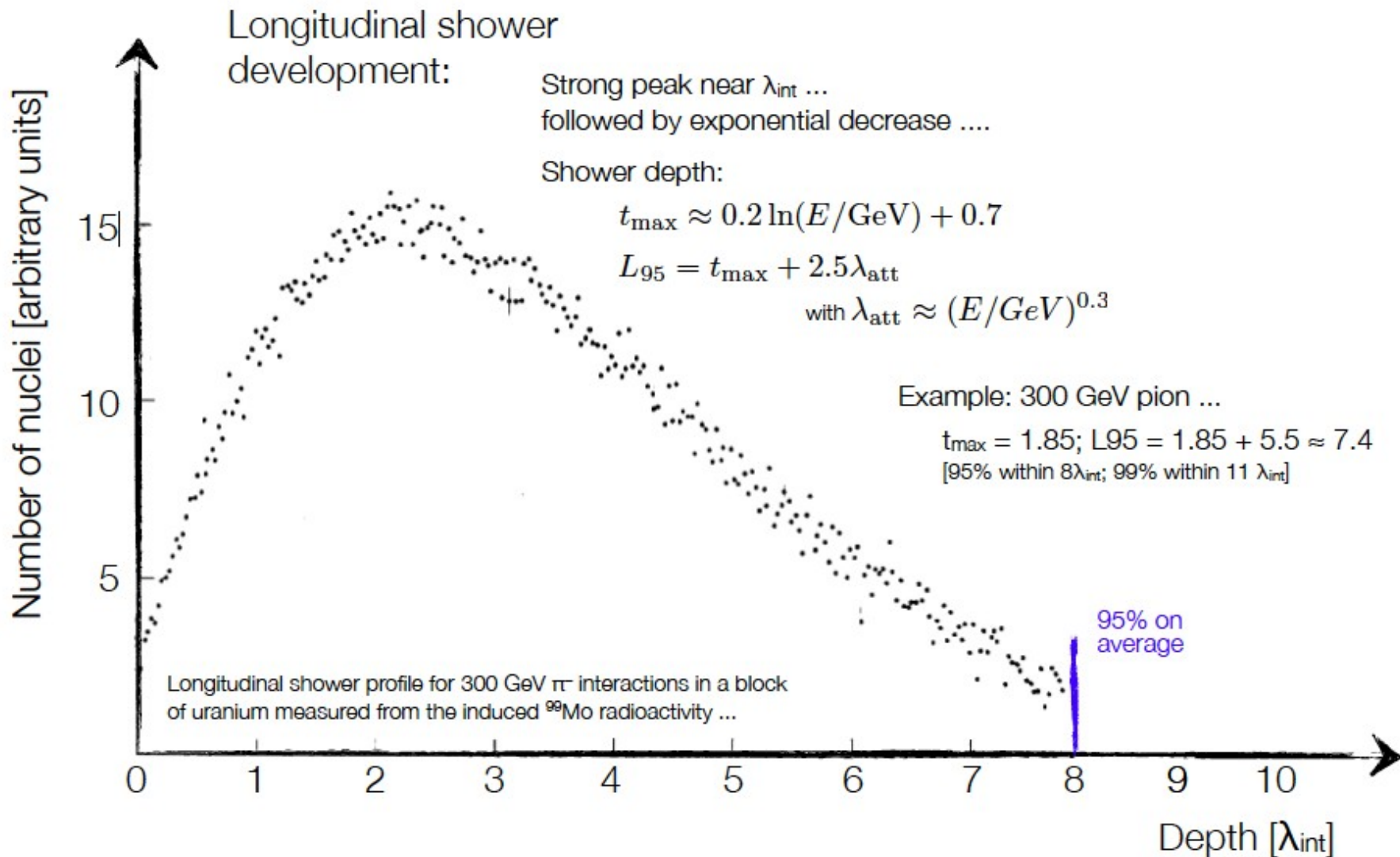
electromagnetic

neutral pions $\rightarrow 2\gamma$ \rightarrow electromagnetic
cascade

number of neutral pions

$$n(\pi^0) \approx \ln E(\text{GeV})$$

for 100 GeV pp collision: $n(\pi^0) \sim 4.6$



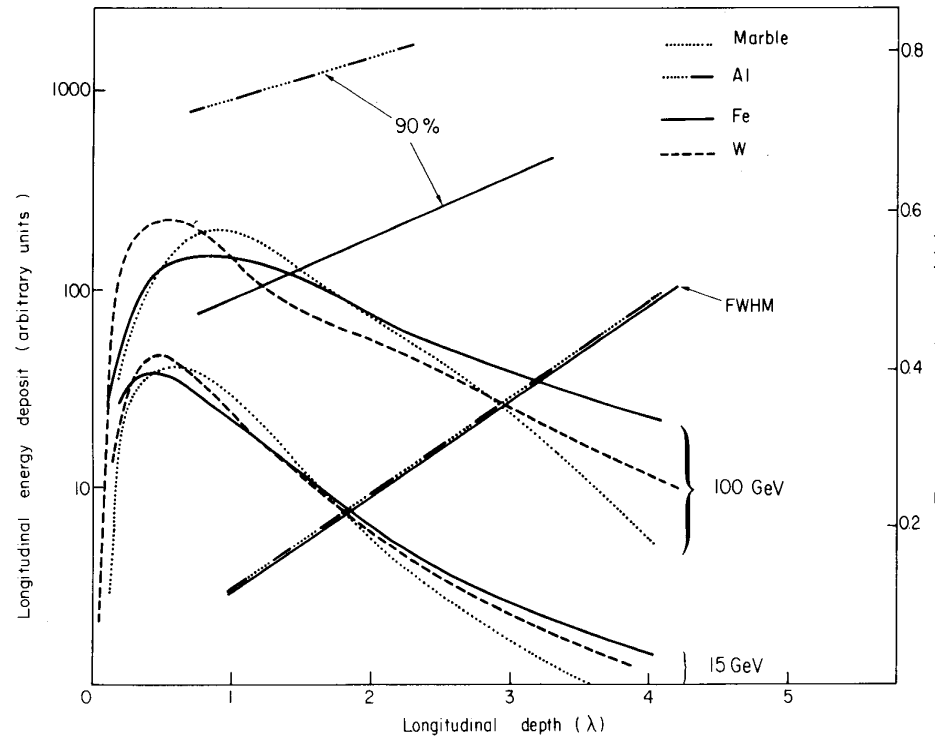
Shower development

Longitudinal shower shape

$$t_{\max}(\lambda_I) \approx 0.2 \ln E[GeV] + 0.7$$

$$t_{95\%}(cm) \approx a \ln E + b$$

For Iron: $a = 9.4$, $b = 39$ $I_a = 16.7 \text{ cm}$
 $E = 100 \text{ GeV}$ $t_{95\%} \sim 80 \text{ cm}$

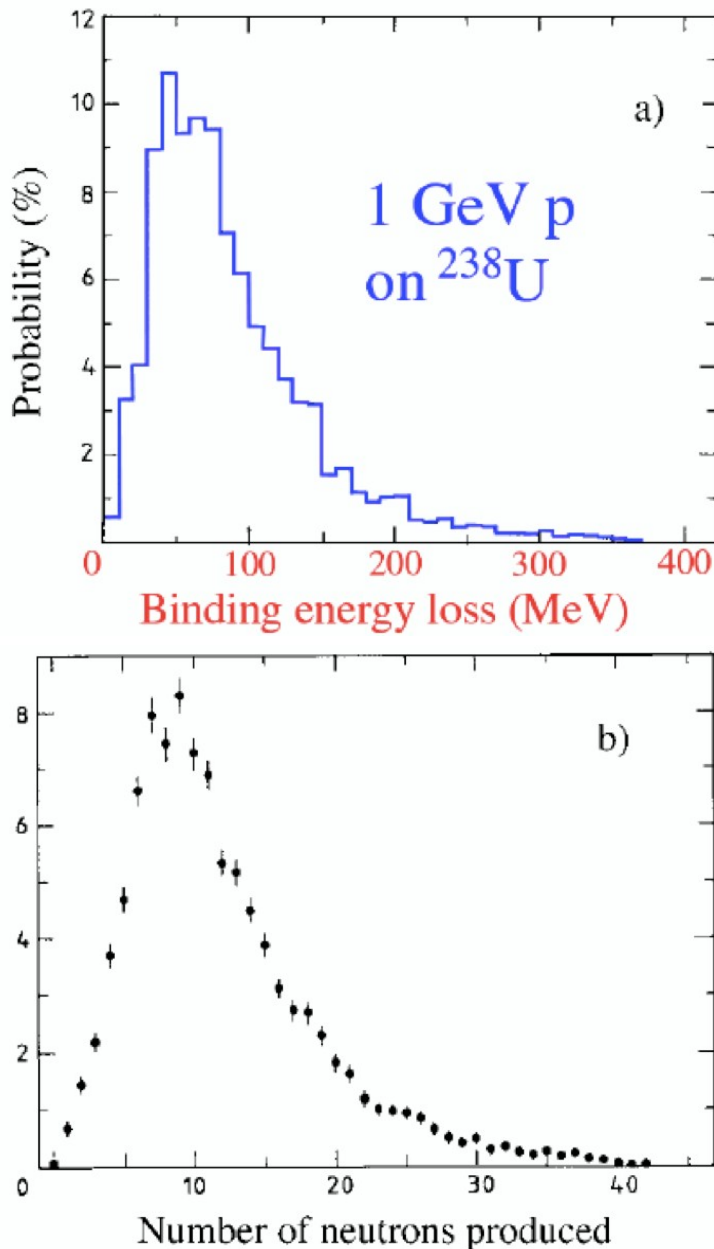


Lateral shower shape

The shower consists of core + halo. 95% containment in a cylinder of radius I_a .
Hadronic showers are much longer and broader than electromagnetic ones

Energy resolution of hadronic showers

- Fluctuations in visible energy (ultimate limit of hadronic energy resolution)
 - fluctuations of nuclear binding energy loss in high-Z materials $\sim 15\%$
- Fluctuations in the EM shower fraction, f_{em}
 - Dominating effect in most hadron calorimeters ($e/h > 1$)
 - Fluctuations are asymmetric in pion showers
 - Differences between p , π induced showers (No leading π^0 in proton showers)
- Sampling fluctuations only minor contribution to hadronic resolution in non-compensating calorimeter



Resolution in EM sampling calorimeters

Main contribution: sampling fluctuations, from variations in the number of charged particles crossing the active layers.

- Increases linearly with incident energy and with the fineness of the sampling.
- Thus:
 $n_{ch} \propto E / t$ where (t is the thickness of each absorber layer)
- For statistically independent sampling the sampling contribution to the stochastic term is:

$$\frac{\sigma_{samp}}{E} = \frac{1}{\sqrt{n_{ch}}} \propto \sqrt{\frac{t}{E}}$$

Thus the resolution improves as t is decreased.

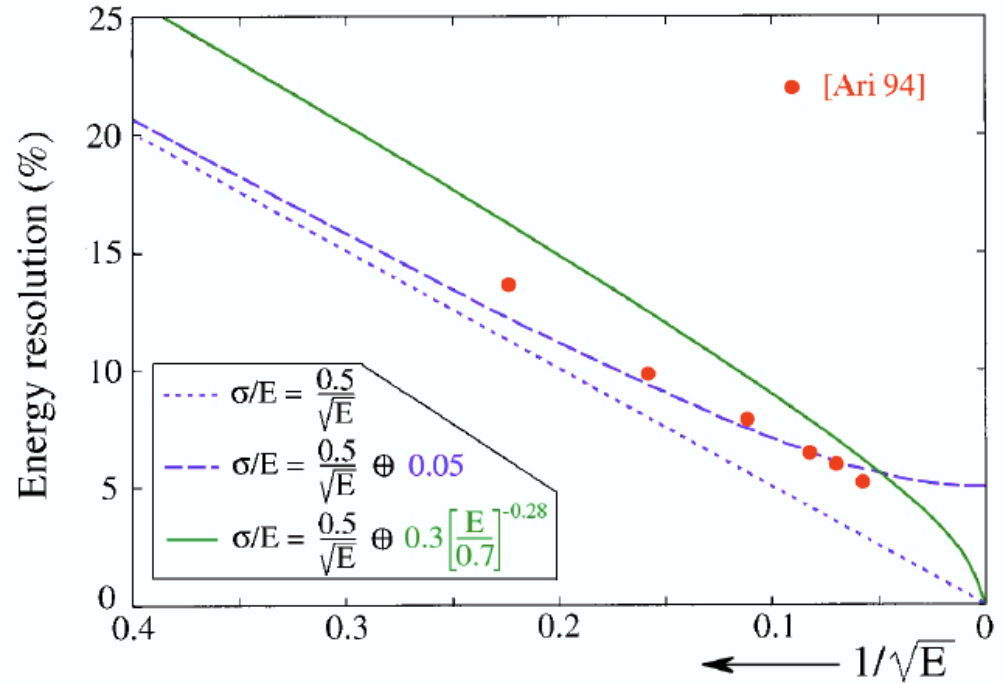
- For EM calorimeters the 100 samplings required to approach the resolution of homogeneous devices is not feasible
- **Typically**

$$\frac{\sigma_{samp}}{E} = \frac{10\%}{\sqrt{E}}$$

Energy resolution of hadron showers

Hadronic energy resolution of non-compensating calorimeters does not scale with $1/\sqrt{E}$ but as

$$\frac{\sigma_E}{E} = \frac{a}{\sqrt{E}} \oplus b \left(\frac{E}{E_0} \right) \approx \frac{a}{\sqrt{E}} \oplus b$$



EM fraction in hadronic calorimeters

The origin of the non-compensation problems

Charge conversion of $\pi^{+/-}$ produces electromagnetic component of hadronic shower (π^0) $\pi^+ n \rightarrow \pi^0 p$

- e = response to the EM shower component
- h = response to the non-EM component

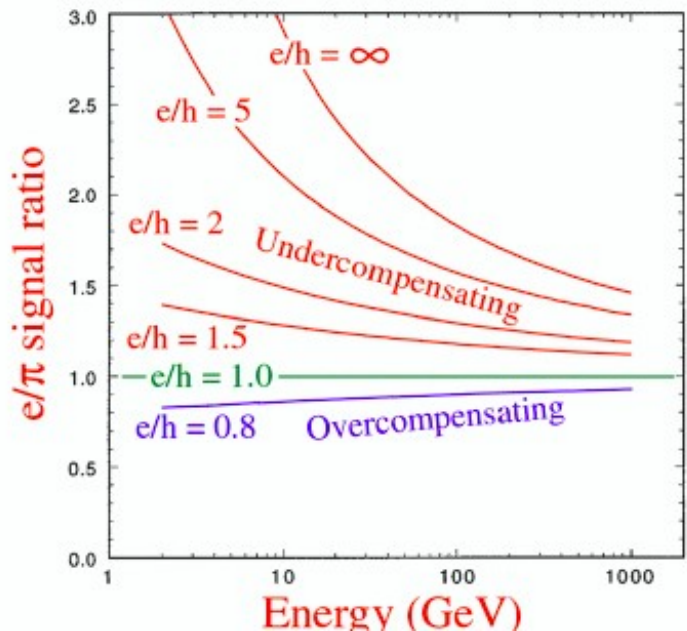
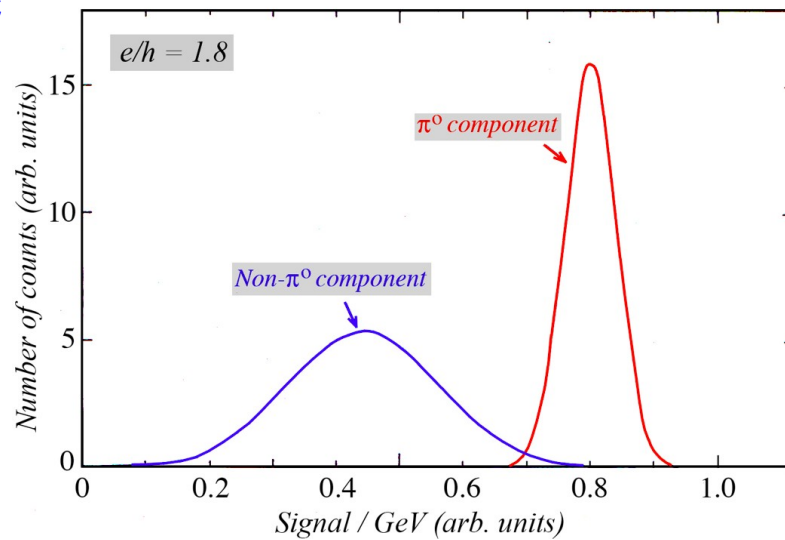
$$\pi = f_{\text{em}} e + (1-f_{\text{em}}) h$$

Comparing pion and electron showers:

$$\frac{e}{\pi} = \frac{e}{f_{\text{em}} e + (1-f_{\text{em}}) h} = \frac{e}{h} \cdot \frac{1}{1 + f_{\text{em}}(e/h - 1)}$$

Calorimeters can be:

- Overcompensating $e/h < 1$
- Undercompensating $e/h > 1$
- Compensating $e/h = 1$



Compensation

Non-linearity determined by e/h value of the calorimeter

- Measurement of non-linearity is one of the methods to determine e/h
- Assuming linearity for EM showers, $e(E_1)=e(E_2)$:

$$\frac{\pi(E_1)}{\pi(E_2)} = \frac{f_{\text{em}}(E_1) + [1 - f_{\text{em}}(E_1)] \cdot e/h}{f_{\text{em}}(E_2) + [1 - f_{\text{em}}(E_2)] \cdot e/h}$$

For $e/h=1 \Rightarrow$

$$\frac{\pi(E_1)}{\pi(E_2)} = 1$$

- Response of calorimeters is usually higher for electromagnetic (e) than hadronic (h) energy deposits $\rightarrow e/h > 1$

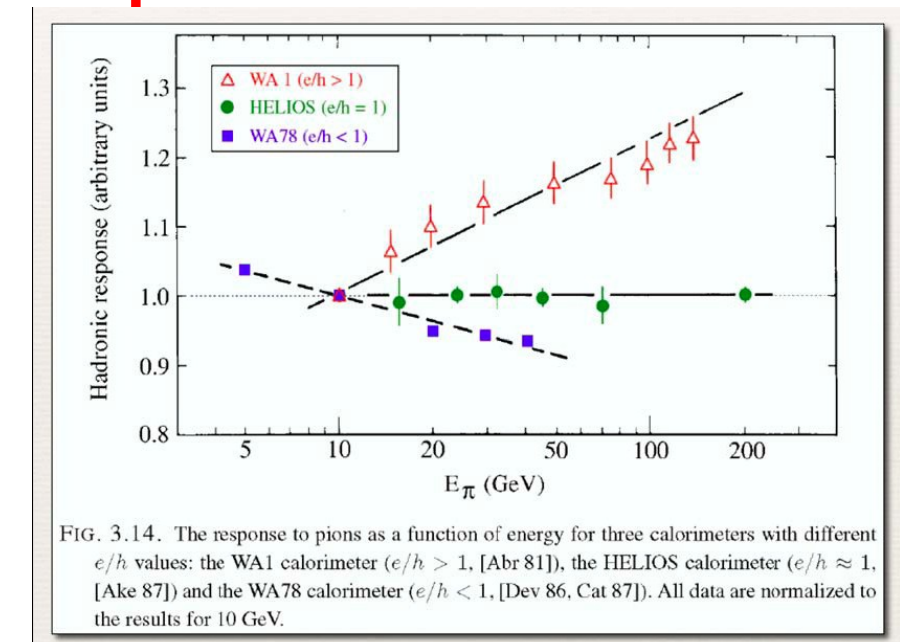
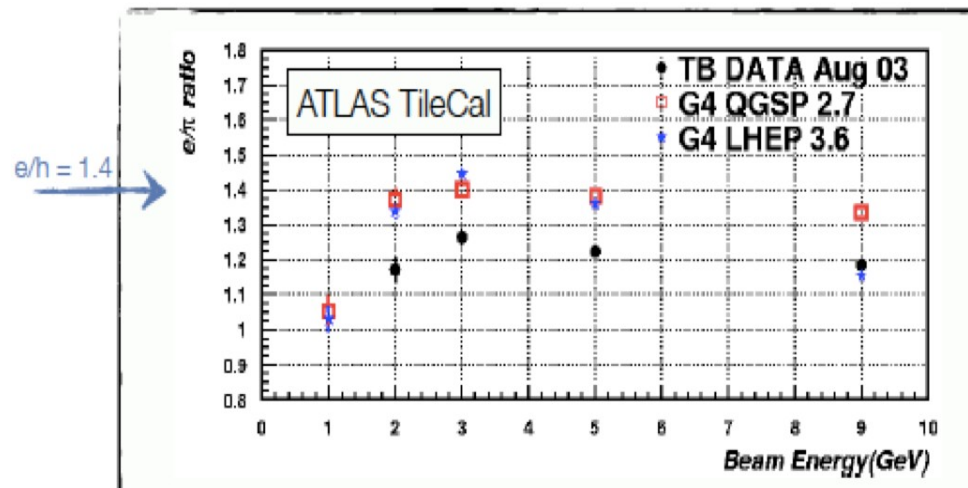
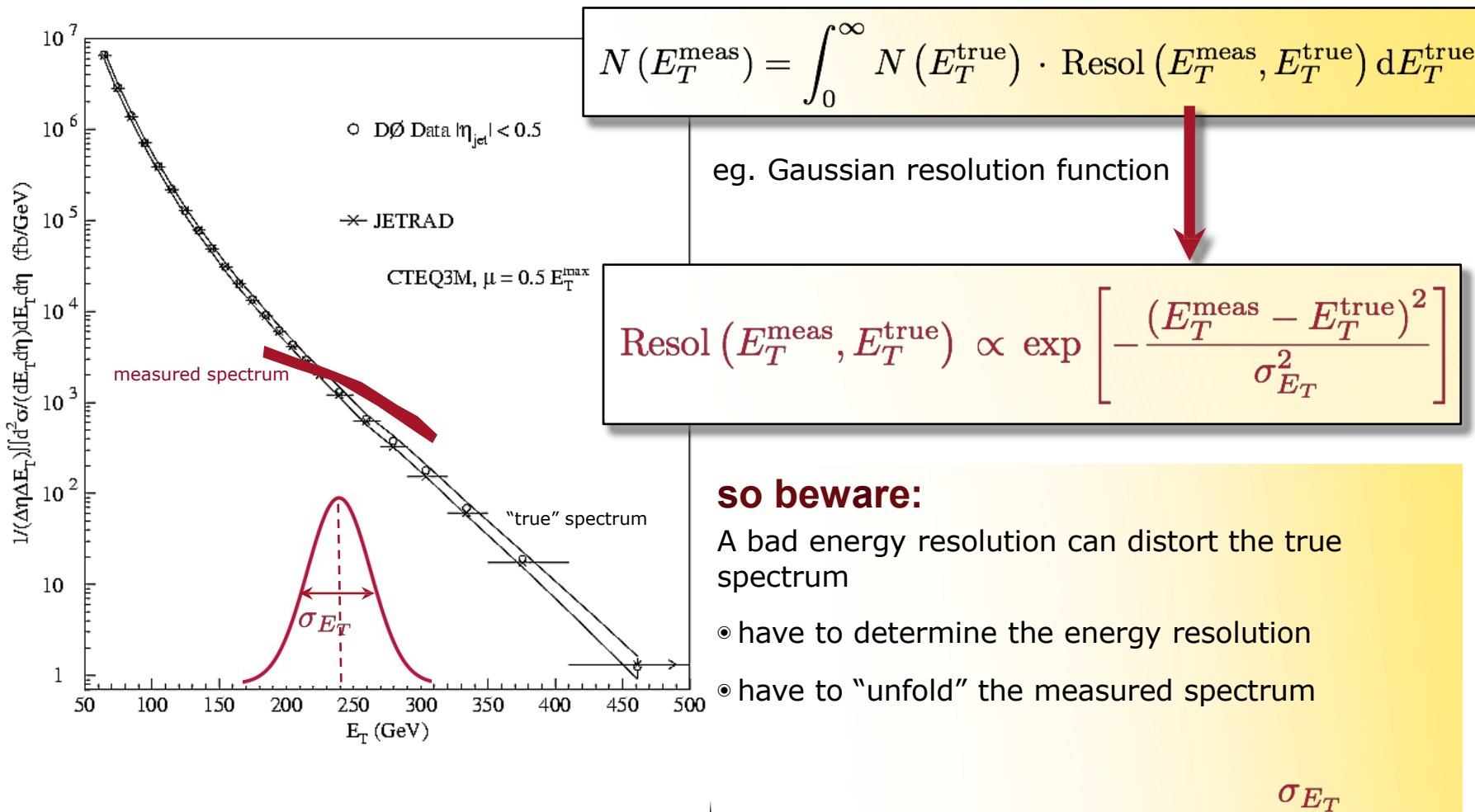


FIG. 3.14. The response to pions as a function of energy for three calorimeters with different e/h values: the WA1 calorimeter ($e/h > 1$, [Abr 81]), the HELIOS calorimeter ($e/h \approx 1$, [Ake 87]) and the WA78 calorimeter ($e/h < 1$, [Dev 86, Cat 87]). All data are normalized to the results for 10 GeV.



Energy resolution

- The **energy resolution** can distort the spectrum
- Again : Critical because of very steeply falling spectrum!



Estimated energy in the ECAL:

$$E_{e,\gamma} = F \times \sum_{\text{clusters}} G c_i A_i$$

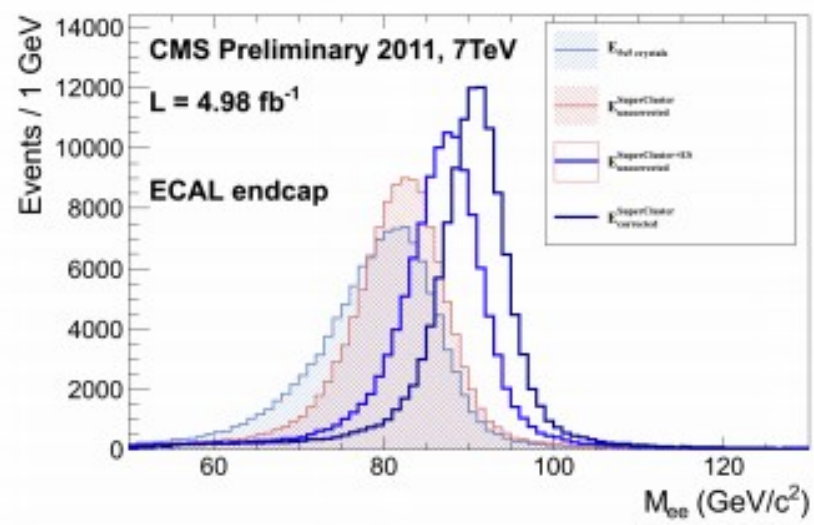
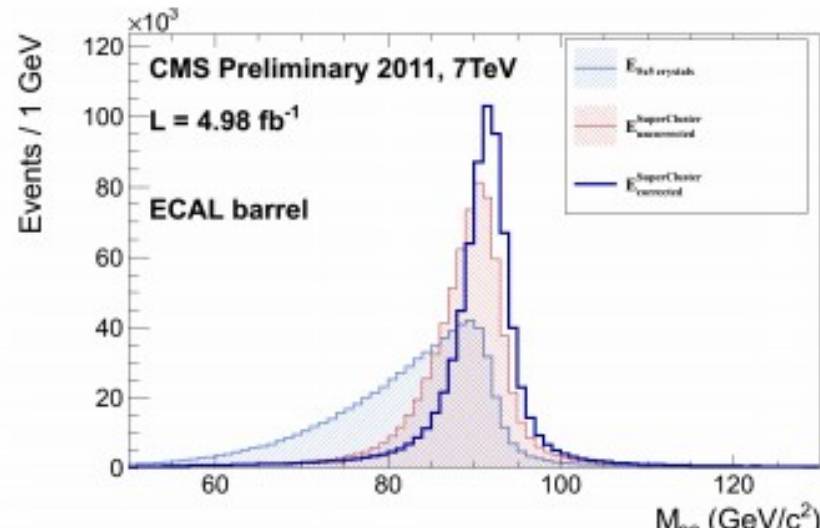
Corrections *Calibration*

Energy correction scheme

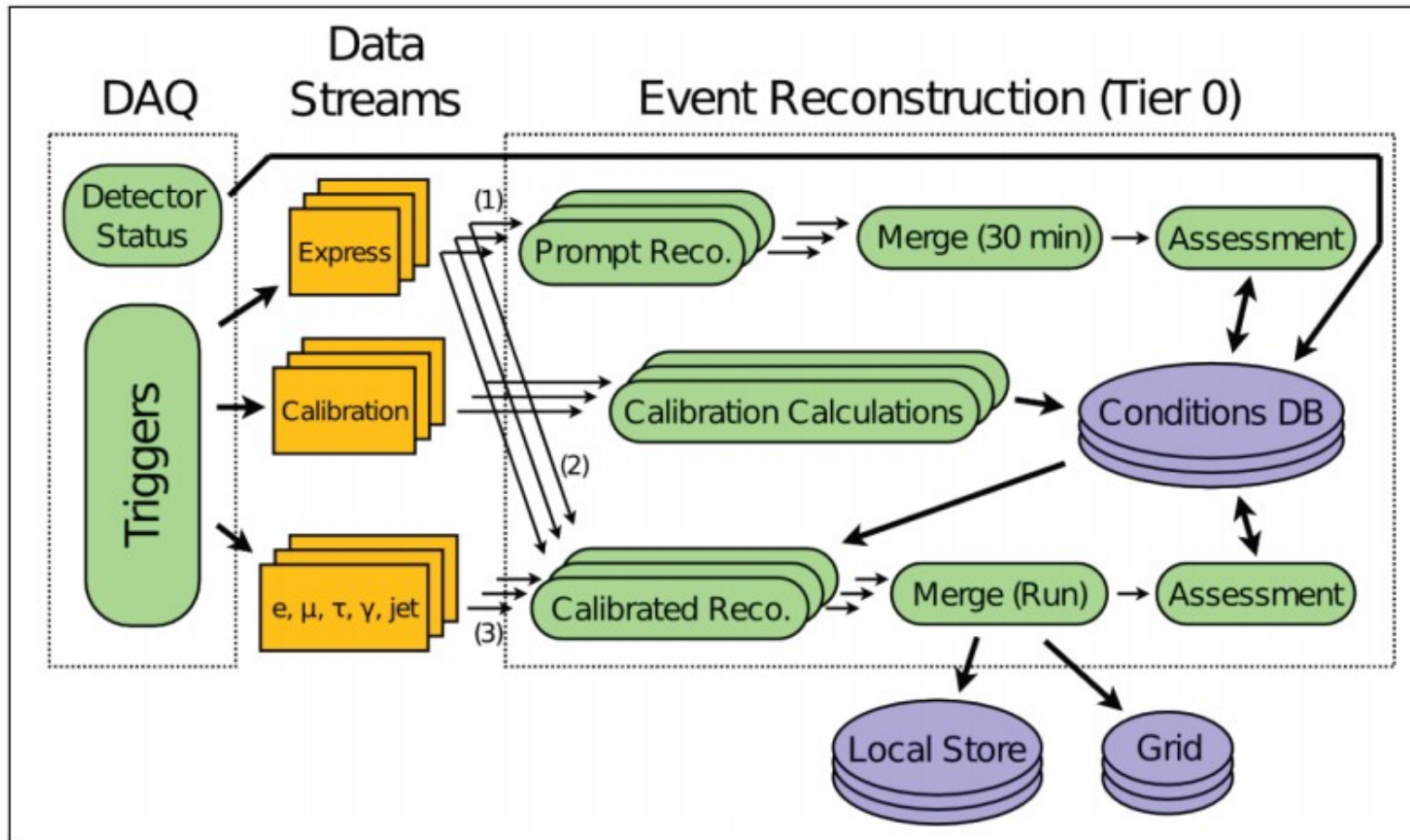
- $F = 1$ for 5x5 crystal sum for the energy of unconverted photons;
- c_i - intercalibration constants (π^0)
- transparency correction with laser monitoring (LM)

ECAL cluster energies corrected using an MC trained multivariate regression

- performed after individual crystal transparency correction and intercalibration
- also provides per photon energy resolution estimate



Prompt reconstruction



In ATLAS we reconstruct the data ~36hours after it is recorded.

This time is used to derive updated calibrations from the data, that are needed in the reconstruction.

Once a year we reprocess all the data with updated software and calibrations.